

Lecture 3.

Applications of x-ray spectroscopy to inorganic chemistry

1. Bioinorganic chemistry/enzymology
2. Organometallic Chemistry
3. Battery materials

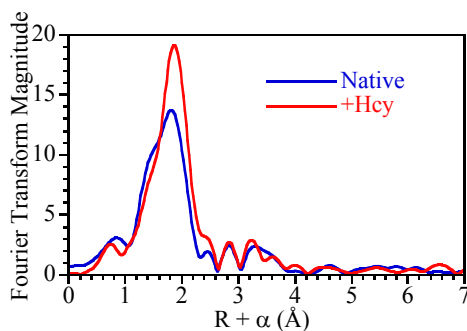
MetE (cobalamin independent MetSyn) contains Zn

Zn is tightly bound

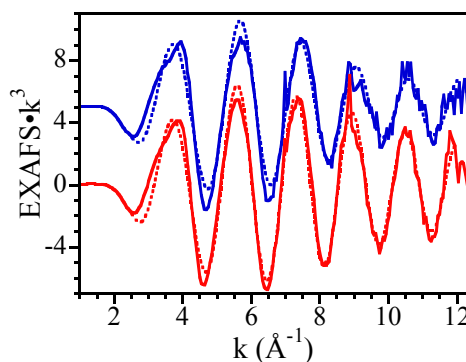
Zn is required for activity

Is Zn involved in reaction, or does it play a
structural role?

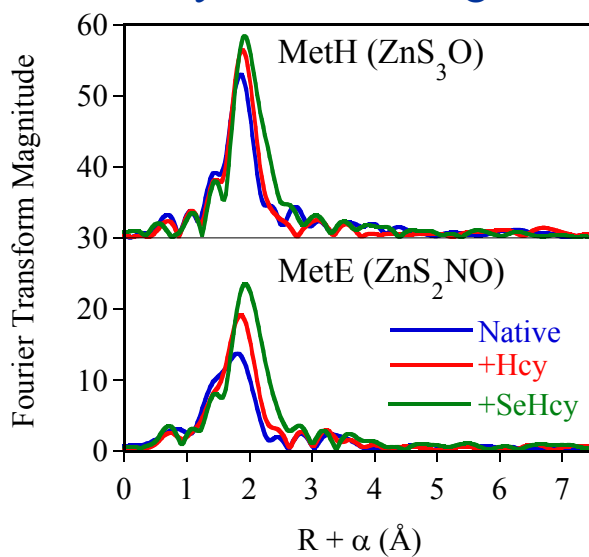
The Zn site in MetE has $\text{ZnS}_2(\text{O/N})_2$ ligation.



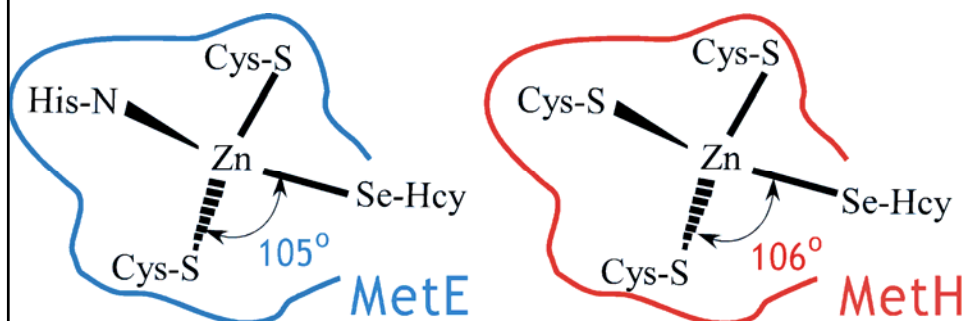
Addition of homocysteine changes ligation to $\text{ZnS}_3(\text{O/N})$.



Changes in ligation are due to homocysteine binding to Zn



Combination of Zn + Se EXAFS consistent with only a small distortion from tetrahedral geometry in substrate-bound enzyme



J. Am. Chem. Soc., **112** (10) 1990

p. 4031-4032

“Higher Order” Cyanocuprates $R_2Cu(CN)Li_2$: Discrete Reagents or “Lower Order” LiCN-Modified Gilman Cuprates?

Bruce H. Lipshutz,* Sunaina Sharma, and Edmund L. Ellsworth†

as $R_2CuLi \cdot LiCN$. We now describe, using spectroscopic studies, prima facie evidence in support of HO cyanocuprates.

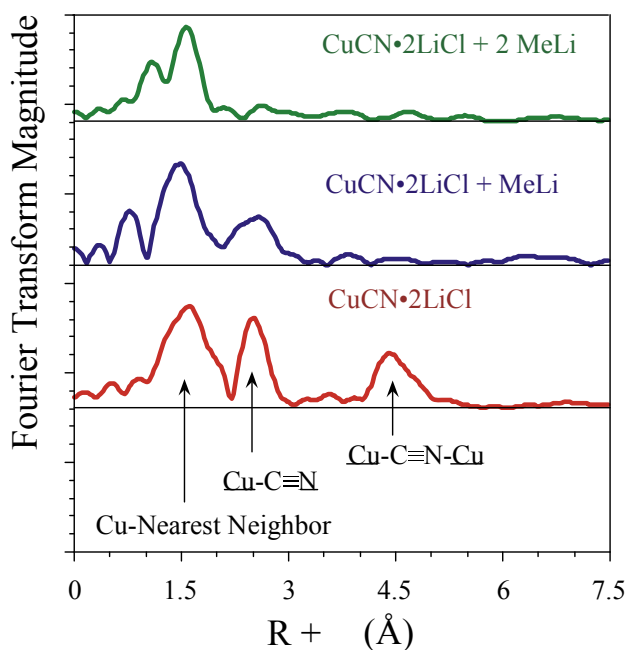
p. 4032-4034

“Higher-Order” Cyanocuprates: Are They Real?¹

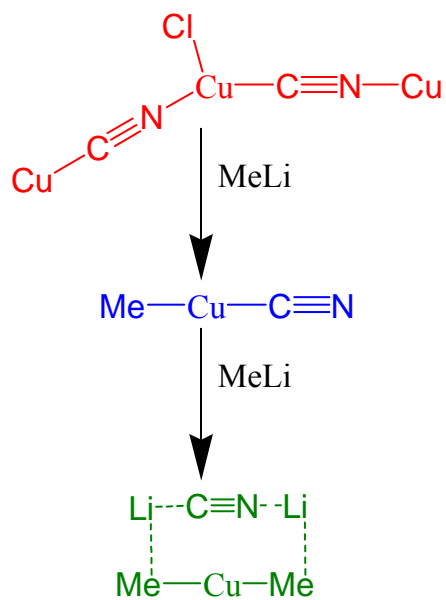
Steven H. Bertz

It can now be reported that the reagents prepared from 2 equiv of RLi (R = alkyl or aryl) and 1 equiv of CuCN may not be truly higher order ate complexes of Cu. ^{13}C NMR spectral evidence

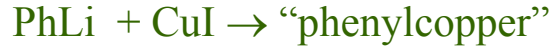
EXAFS
shows
that CN^-
does not
remain
bound



Structures of cyanocuprates in THF



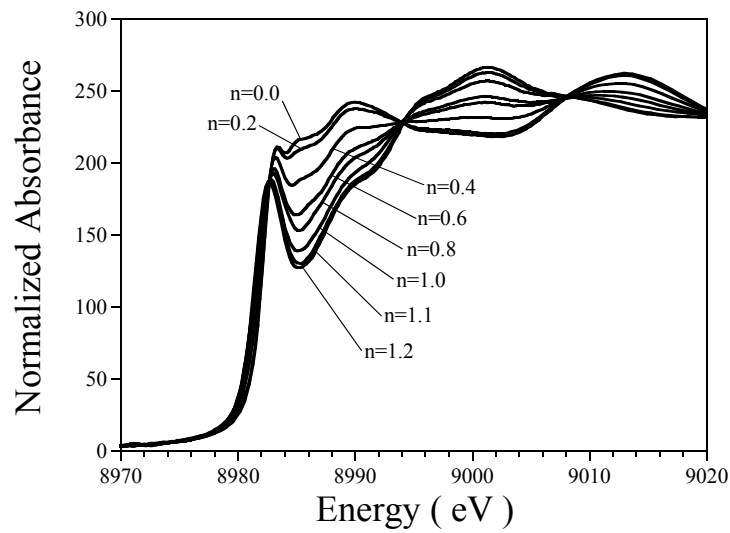
Solution speciation of CuI+PhLi



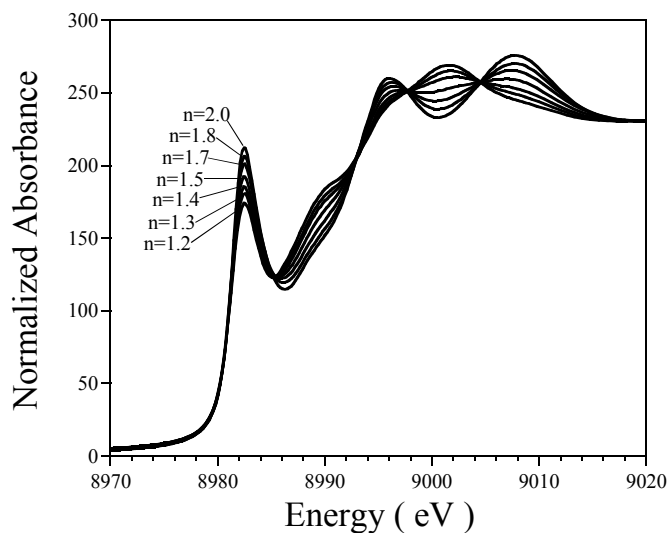
Crystalline phenyl:copper species

| | | | |
|-------|---|-----|---|
| 1:1 | $\text{Cu}_4\text{Ph}_4(\text{Me}_2\text{S})_2$ | 2:1 | $[\text{CuPh}_2]^-$ |
| | Cu_5Mes_5 | | $[\text{CuPh}_2\text{Li}]_2$ |
| 1.2:1 | $[\text{Cu}_5\text{Ph}_6]^-$ | | $[\text{Cu}_3\text{Li}_2\text{Ph}_6]^-$ |
| 1.5:1 | $[\text{Cu}_4\text{LiPh}_6]^-$ | | |
| | $[\text{Cu}_4\text{MgPh}_6]$ | | |

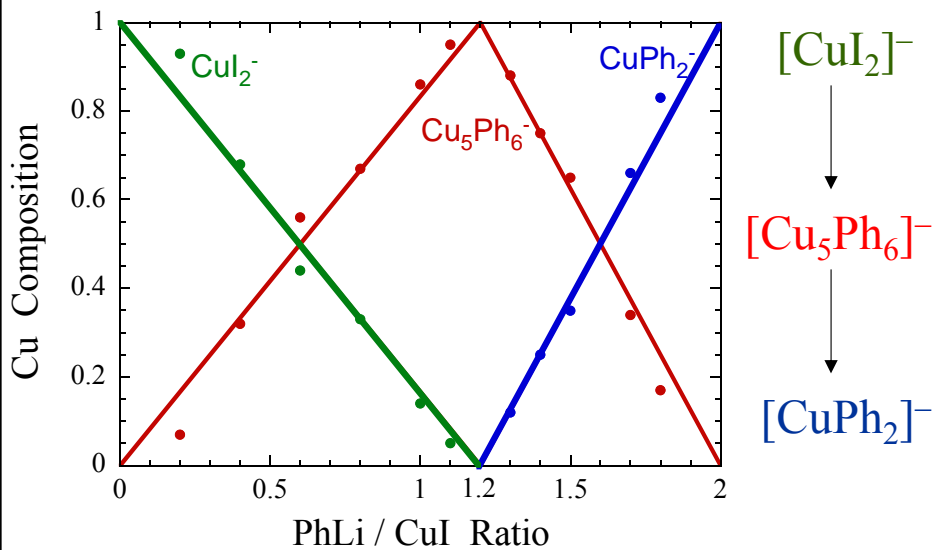
Titration of CuI+ *n* PhLi shows isosbestic behavior up to 1.2 equivalents



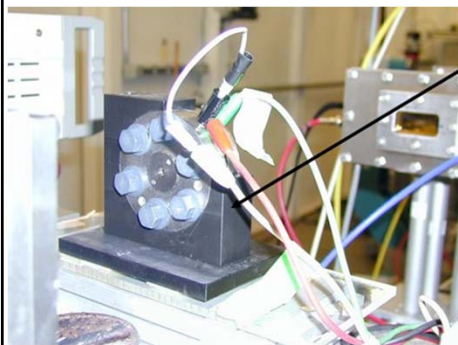
Titration of $\text{CuI} + n \text{ PhLi}$ shows isosbestic behavior from 1.2-2.0 equivalents



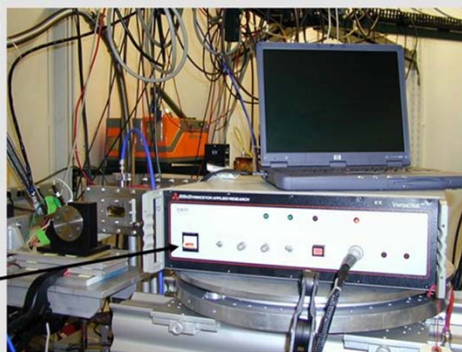
EXAFS data support XANES speciation



In-situ X-ray Absorption Spectroscopy



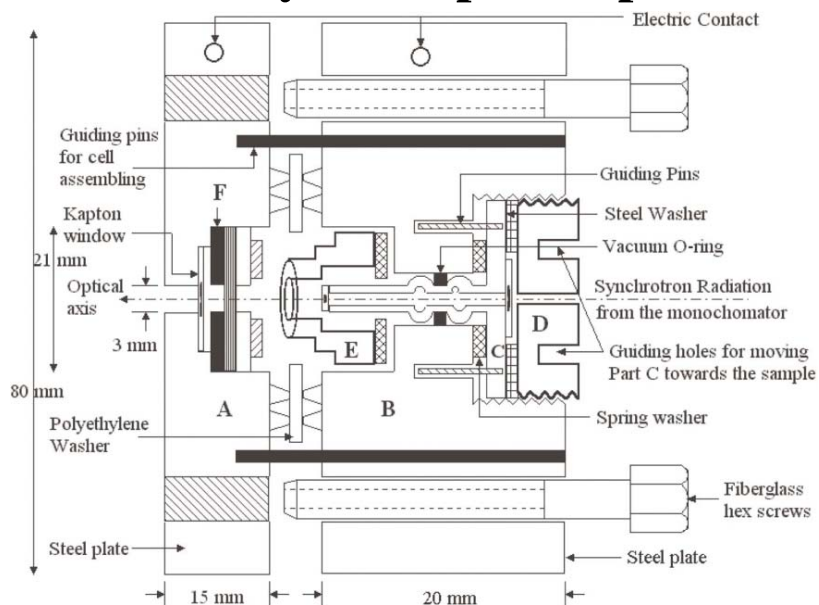
Electrochemical Cell connected to potentiostat at the Beamline



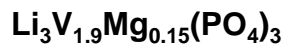
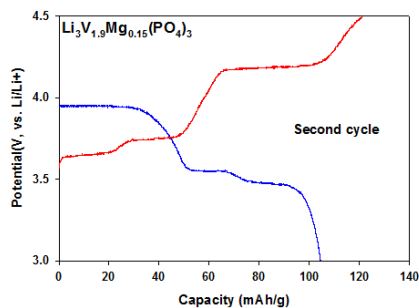
Cycling of the cell using potentiostat

Aniruddha Deb et al. J. Synchrotron Rad. (2004). 11, 497–504

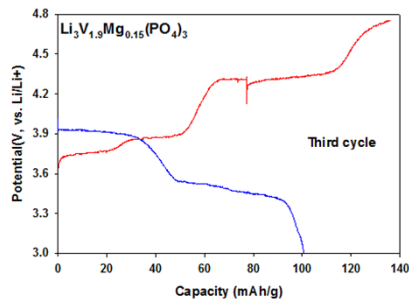
In-situ X-ray Absorption Spectroscopy



Charge/Discharge at 0.1C

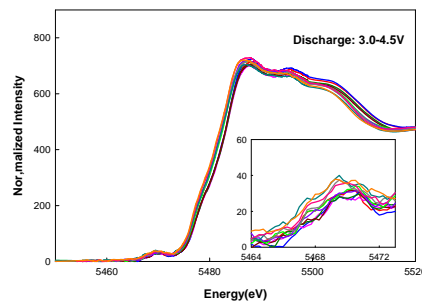
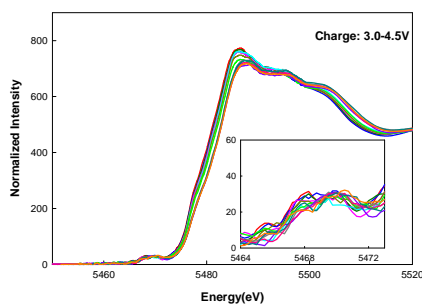


- Cut off : **3.0 V-4.5V**
- Charge: 121 mAh/g
- Discharge: 104 mAh/g



- Cut off : **3.0 V-4.8V**
- Charge: 136 mAh/g
- Discharge: 100 mAh/g

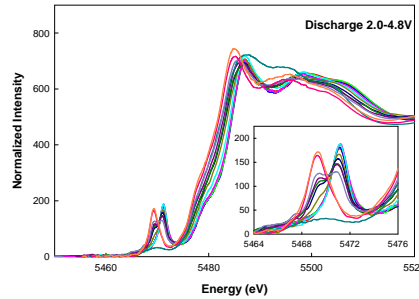
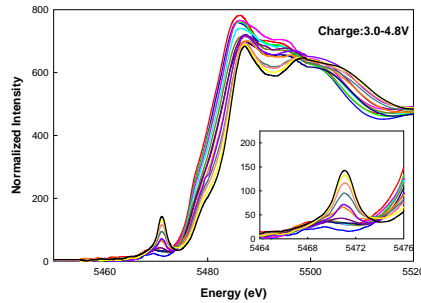
$\text{Li}_3\text{V}_{1.9}\text{Mg}_{0.15}(\text{PO}_4)_3$



Between 3.0-4.5V

- No change shown in the pre-edge region for a cut off of 4.5V
- Between 3-4.5V changes in the edge, observed, showing oxidation state change
- No significant e_g-t_{2g} splitting observed in the pre-edge region
- Octahedral structure preserved

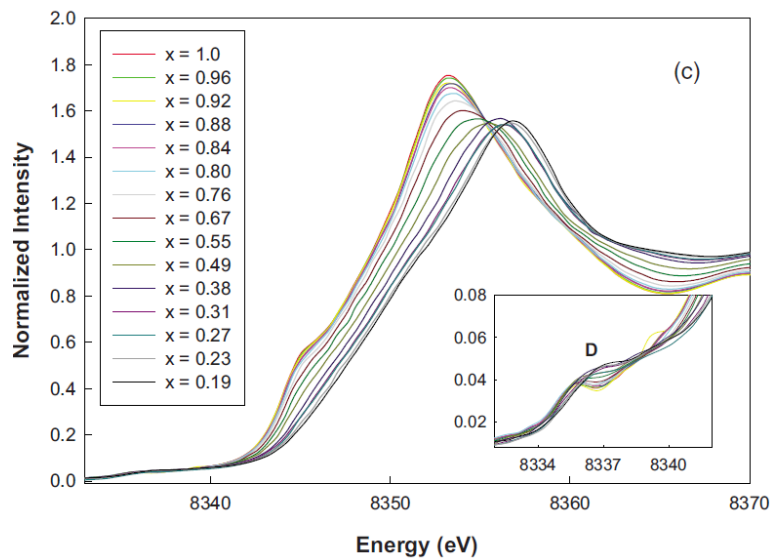
$\text{Li}_3\text{V}_{1.9}\text{Mg}_{0.15}(\text{PO}_4)_3$

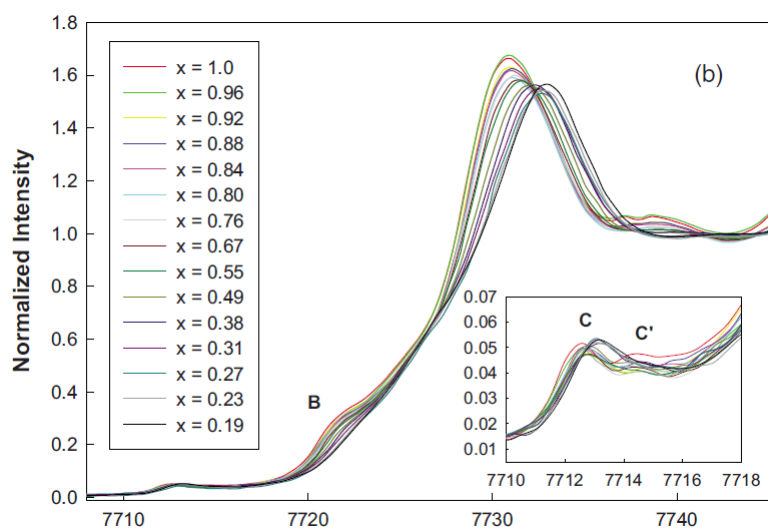
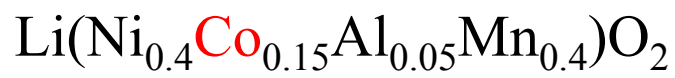
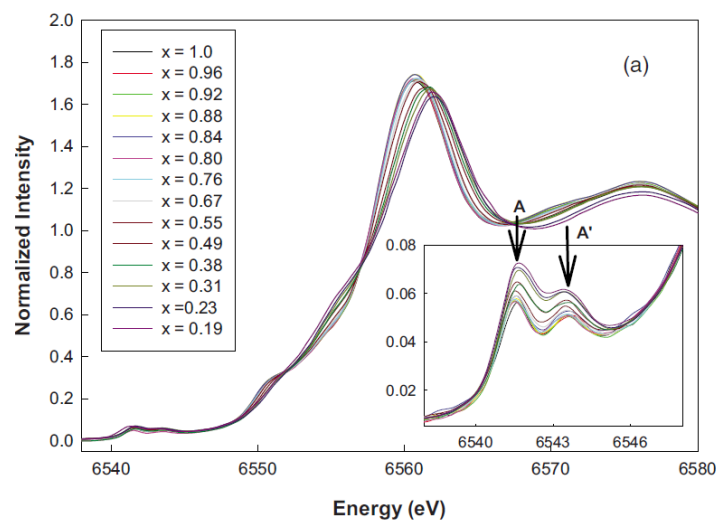
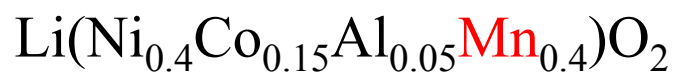


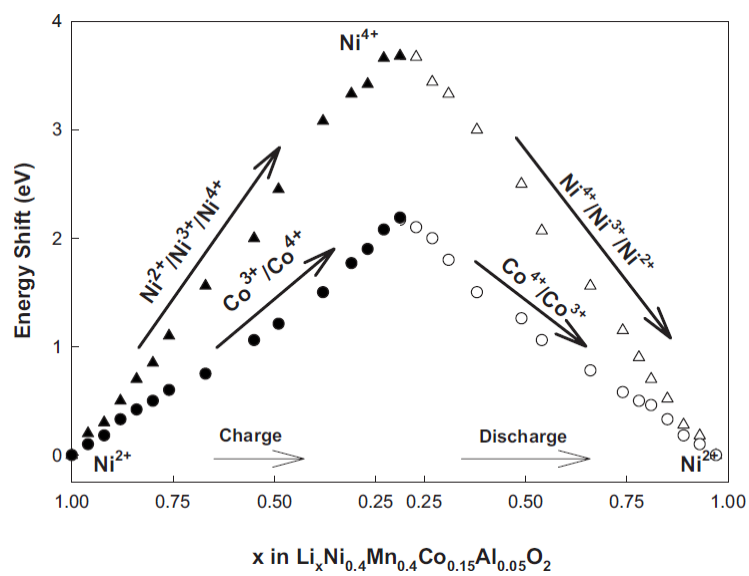
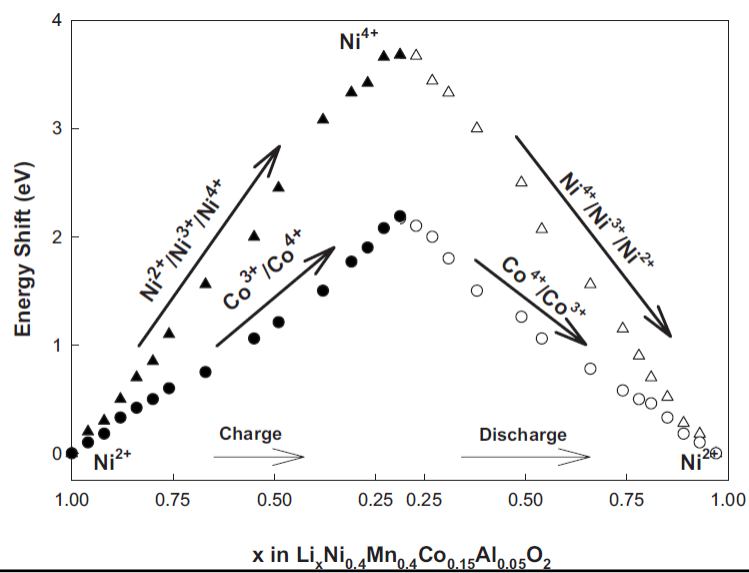
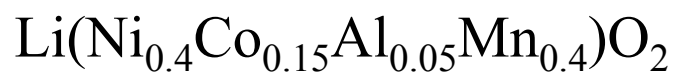
Above 4.5V and below 3.0V

- Above 4.5V change in edge consistent with formation of tetrahedral V^{4+} or V^{5+} .
- XANES change is largely irreversible.
- Possible structural change below 3.0V as the pre-edge intensity increases

$\text{Li}(\text{Ni}_{0.4}\text{Co}_{0.15}\text{Al}_{0.05}\text{Mn}_{0.4})\text{O}_2$





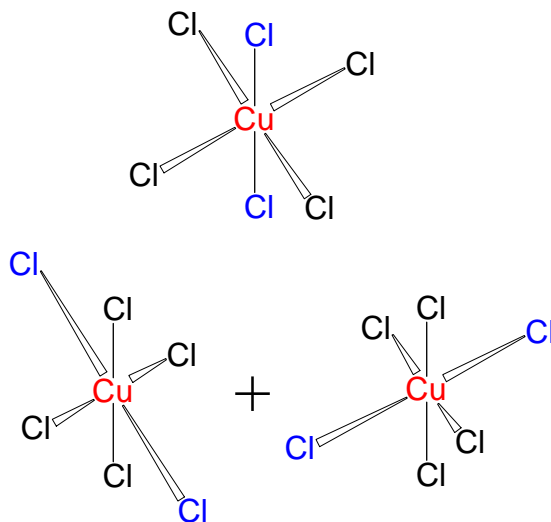


Applications of EXAFS to Crystallographically Characterized Materials

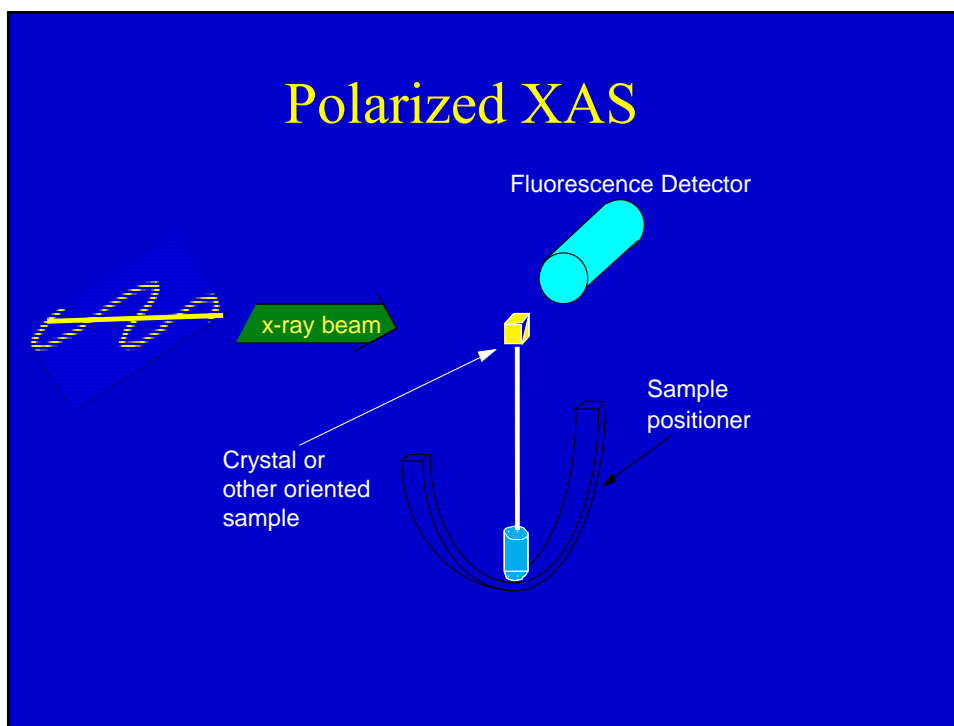
Inorg. Chem. 1994, 33, 1249–1250

EXAFS Evidence That the CuCl_6^{4-} Ion in $(3\text{-Chloroanilinium})_8(\text{CuCl}_6)\text{Cl}_4$ Has an Elongated Rather Than Compressed Tetragonal Geometry

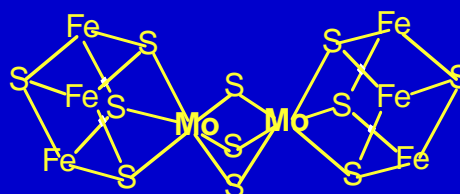
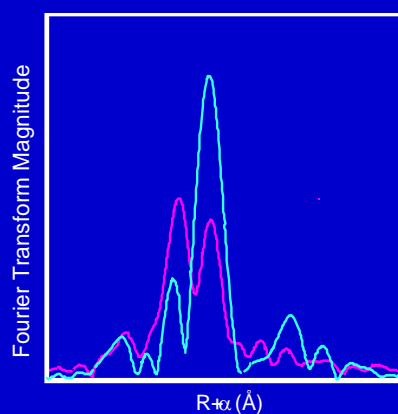
Paul J. Ellis,[†] Hans C. Freeman,^{*†} Michael A. Hitchman,^{*‡} Dirk Reinen,[§] and Burghard Wagner[§]



Polarized XAS



Polarized XAFS of Mo/Fe/S clusters

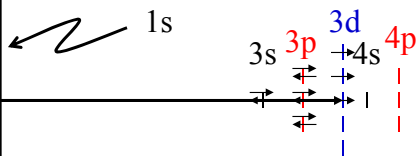
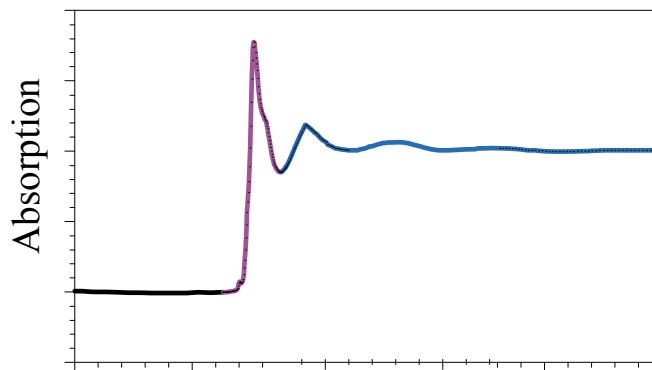


Flank, Weininger, Mortenson, & Cramer, *J. Am. Chem. Soc.*, **108**, 1049.

Examples using XANES to determine electronic structure

X-ray absorption spectroscopy

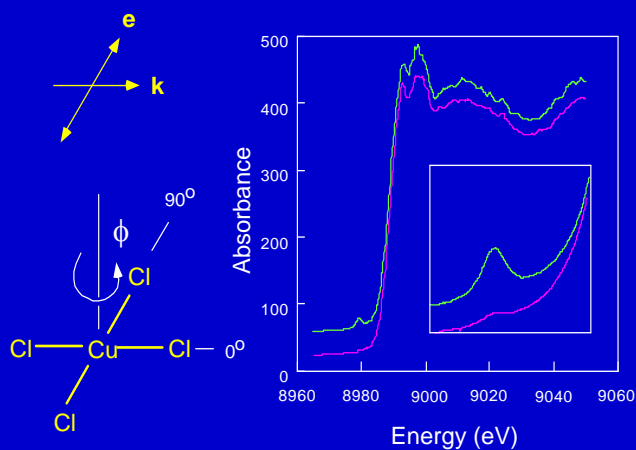
XANES EXAFS



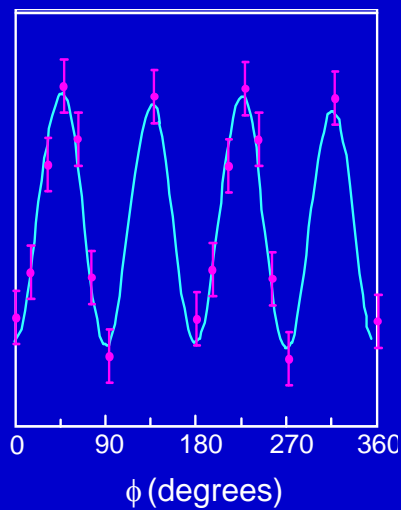
1s→3d transitions

- Dipole forbidden ($\Delta L = 2$) for centrosymmetric complexes
- Weak, but not absent, for all first row transition metals
- Possible mechanisms
 - 3d+4p mixing (not possible for centrosymmetric complexes)
 - vibronic coupling
 - direct quadrupole coupling

Orientation dependence of 1s→3d transition



Four-fold periodicity to $1s \rightarrow 3d$ transition

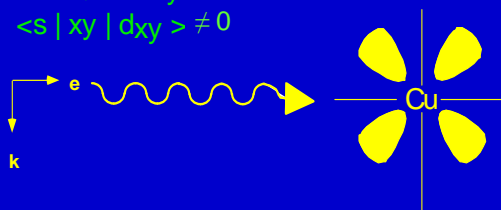


Quadrupole transitions – $\Delta L=2$

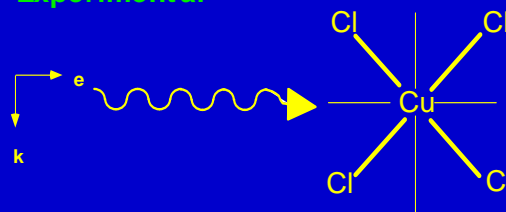
Theoretical

$$\langle s | xy | d_{x^2-y^2} \rangle = 0$$

$$\langle s | xy | d_{xy} \rangle \neq 0$$



Experimental



Selection rules for quadrupole transitions

$$\sigma_{z^2} = 6\sqrt{5} \sin^2 \theta \cos^2 \theta \sin^2 \psi \cdot \zeta_{z^2}$$

$$\sigma_{x^2-y^2} = 2\sqrt{5} \sin^2 \theta [\sin \psi \sin 2\phi - \cos \theta \cos \psi \cos 2\phi]^2 \cdot \zeta_{x^2-y^2}$$

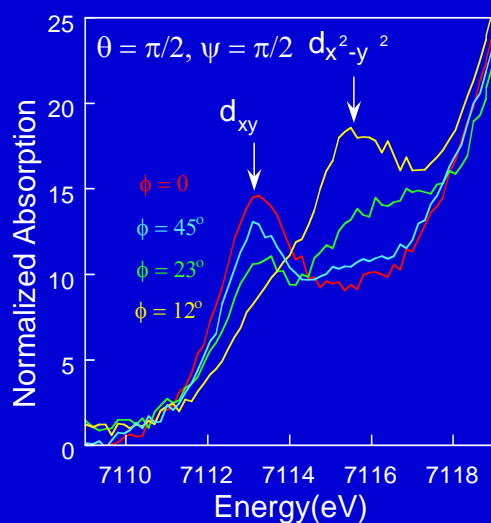
$$\sigma_{xy} = 2\sqrt{5} \sin^2 \theta [\sin \psi \cos 2\phi - \cos \theta \cos \psi \sin 2\phi]^2 \cdot \zeta_{xy}$$

$$\sigma_{yz} = 2\sqrt{5} [\cos \theta \sin \psi \cos \phi - \cos 2\theta \cos \psi \sin \phi]^2 \cdot \zeta_{yz}$$

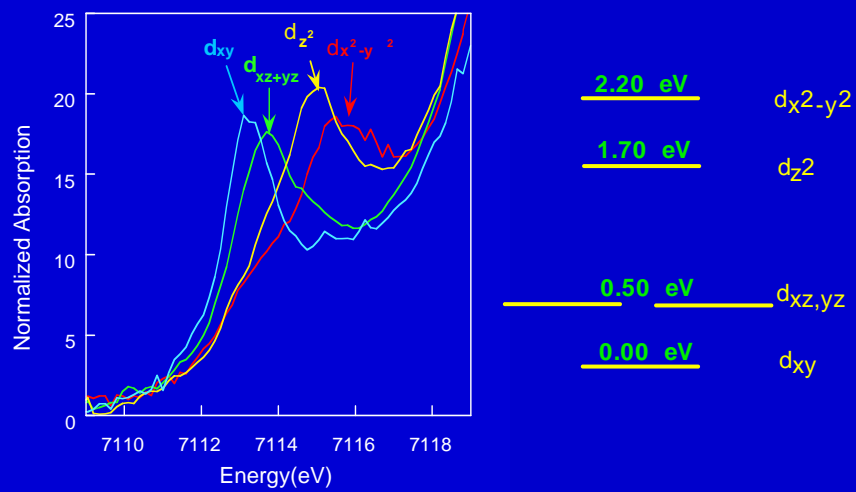
$$\sigma_{xz} = 2\sqrt{5} [\cos \theta \sin \psi \sin \phi - \cos 2\theta \cos \psi \cos \phi]^2 \cdot \zeta_{xz}$$

Brouder, C. *J. Phys. Condens. Matter*, **2** (1990) 701-738

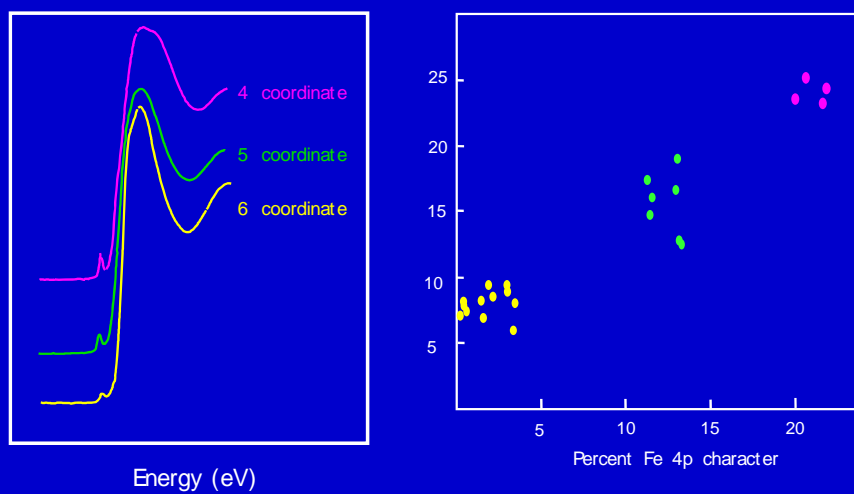
1s→3d transitions for Fe porphyrins



Isolated 1s→3d for Fe(OEP)(2-MeIm)



XANES for Fe(III) complexes



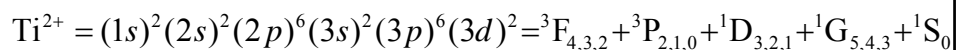
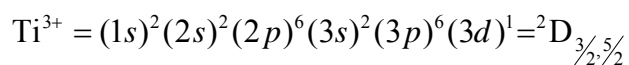
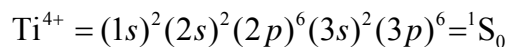
Roe et al., *J. Am. Chem. Soc.*, **106**, 1676

1s→3d intensity

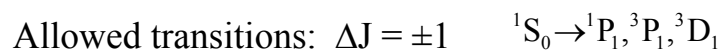
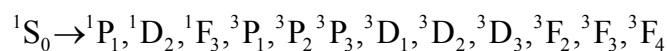
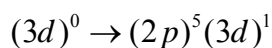
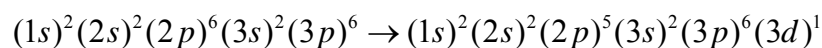
- Weak for square–planar complexes
- Strong for tetrahedral complexes
- Correlates with coordination number

Electronic information
is (often) enhanced by
studying L-edge rather
than K-edge

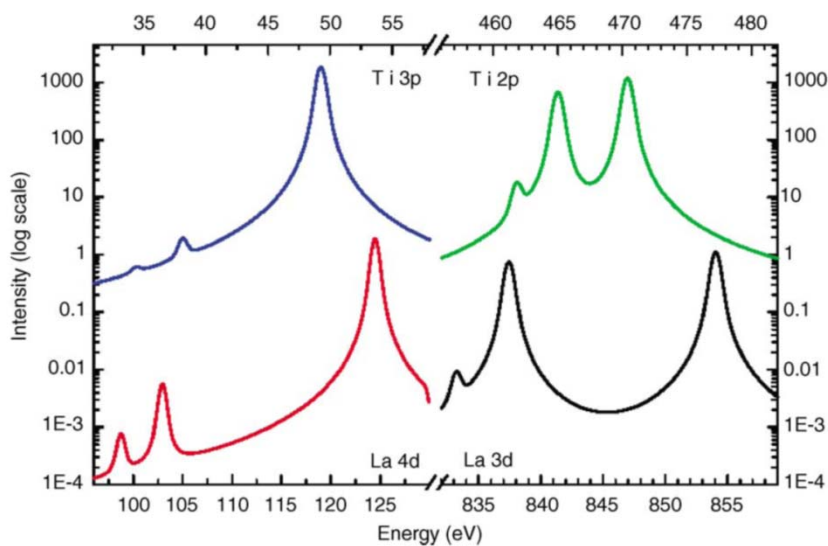
Multiplet effects



L edge of Ti^{4+}

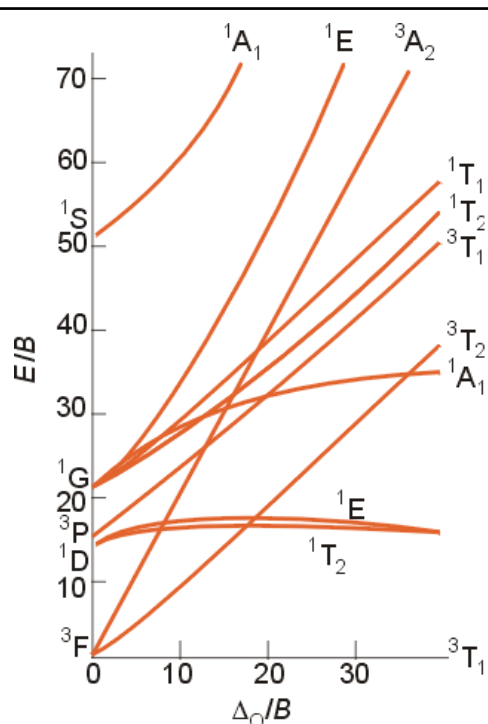


Simulations of L edges

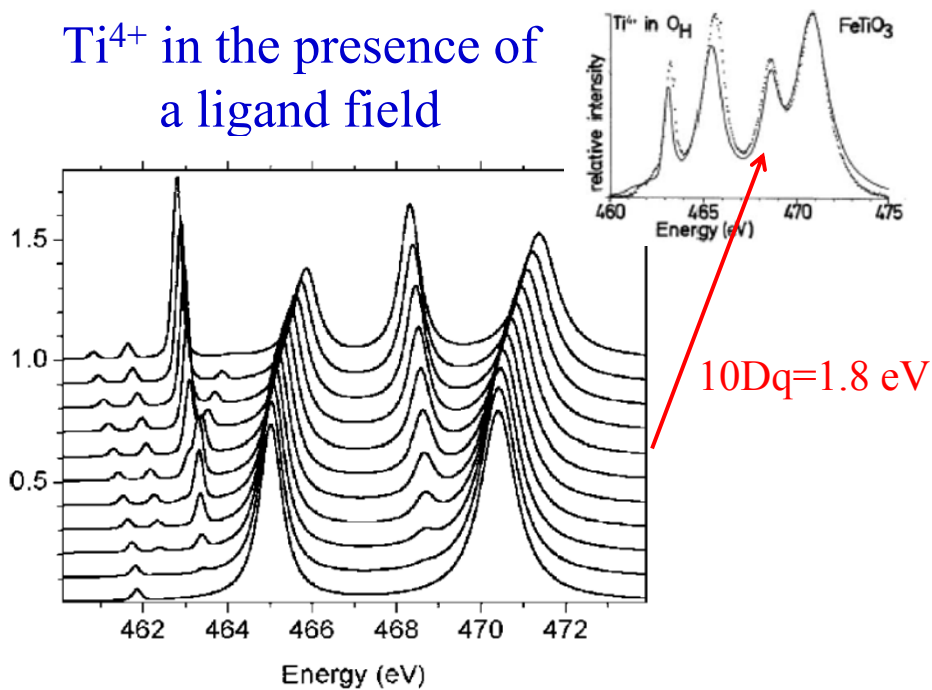


DeGroot, *Coord. Chem. Rev.* **2005**, *249*, 31–63

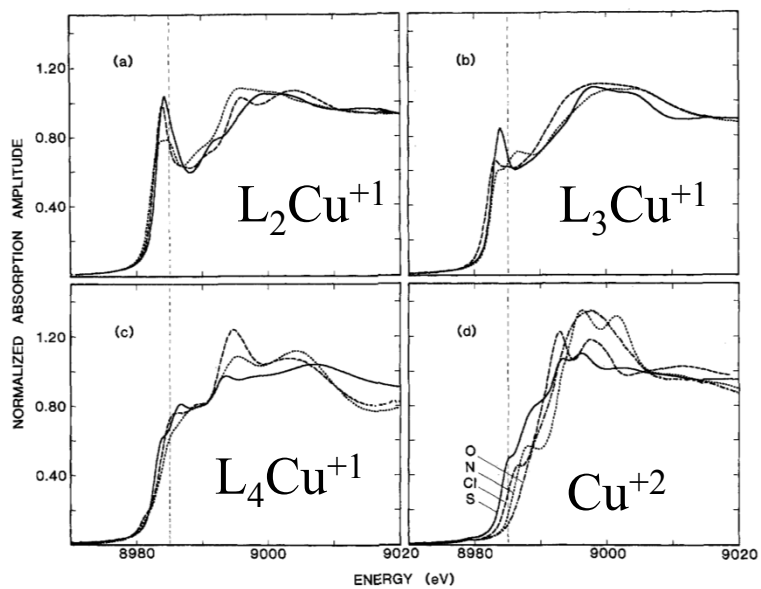
But – life is not really this simple – need to consider ligand field: d^2 terms vs ligand field



Ti^{4+} in the presence of a ligand field

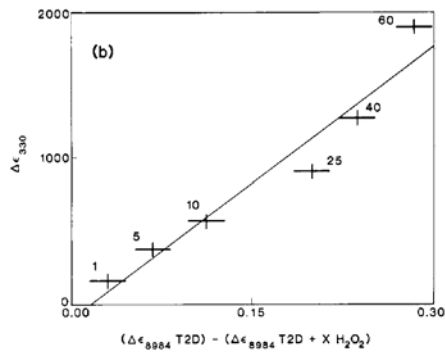
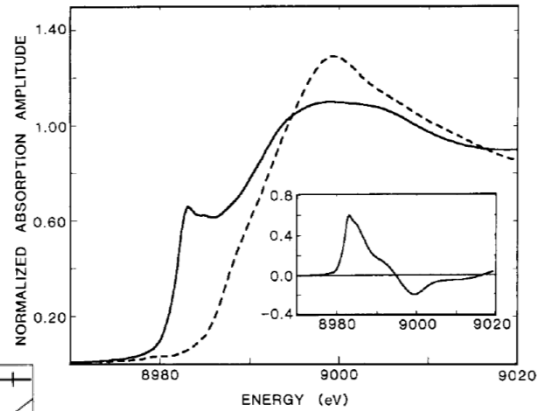


Determination of Oxidation State



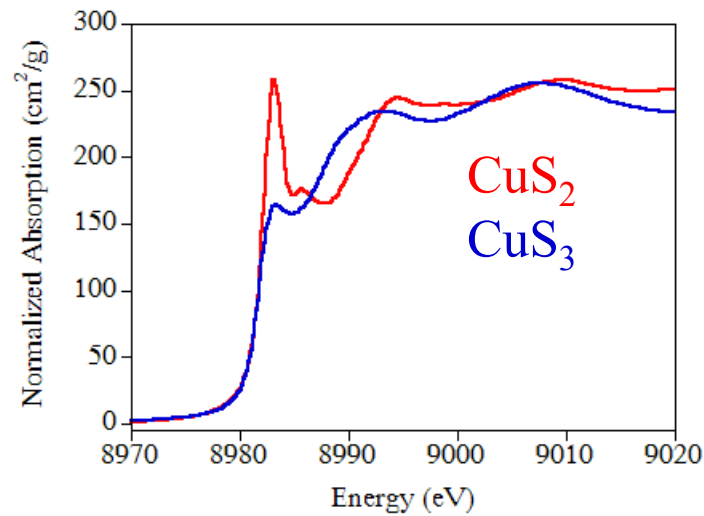
Kau et al., J. Am. Chem. Soc., 1987, 109, 6433

By defining
 “generic” Cu(I)
 and Cu(II)
 XANES



can determine
 change in Cu
 oxidation state

Sensitivity of XANES to geometry is consistent with
 expected density of unoccupied Cu 4p orbitals



Theoretical calculations of XANES

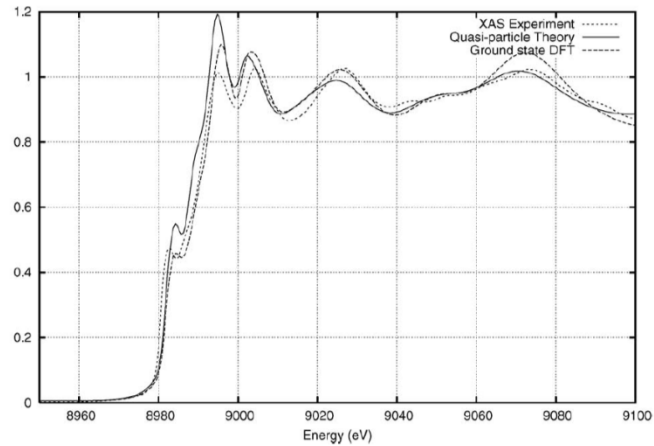
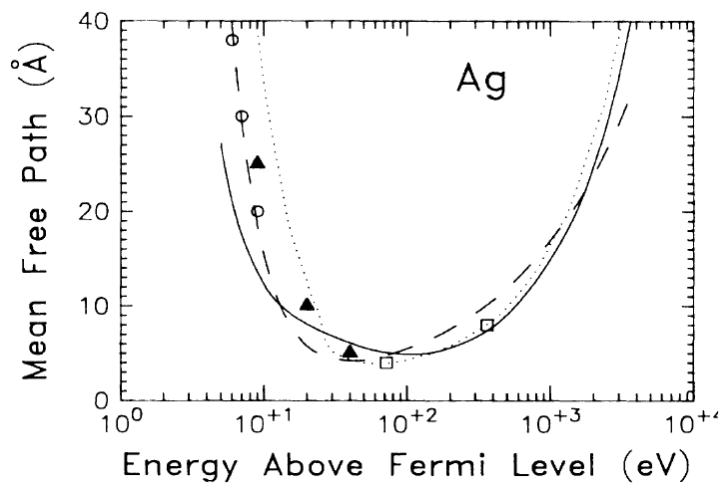


Fig. 1. XANES for K-shell Cu from XAS experiment (dots); from calculations with the FEFFS code using the standard quasi-particle theory including a plasmon-pole self-energy and a screened core-hole (solid line); and from ground state density functional theory without a core-hole (dashes). **Note that ground state theory (without a core-hole) is in reasonable agreement with experiment at the edge, but has too large an amplitude at high energies,** where the standard theory is in reasonable agreement.

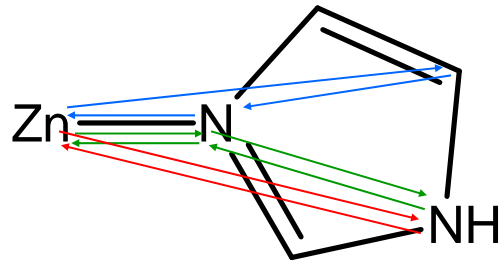
Rehr and Ankudinov, *Coord. Chem. Rev.* **2005**, 249 131–140

Mean-free path increases dramatically for energies near the edge – accounts for some of the difficulty with XANES calculations

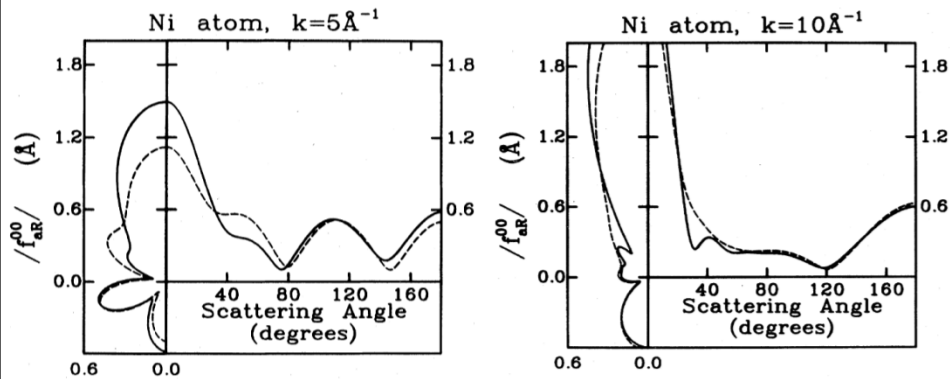


Penn. Phys. Rev. B **35**, 1987 482–486

The difficulty of simulating XANES is also due (in part) to multiple scattering

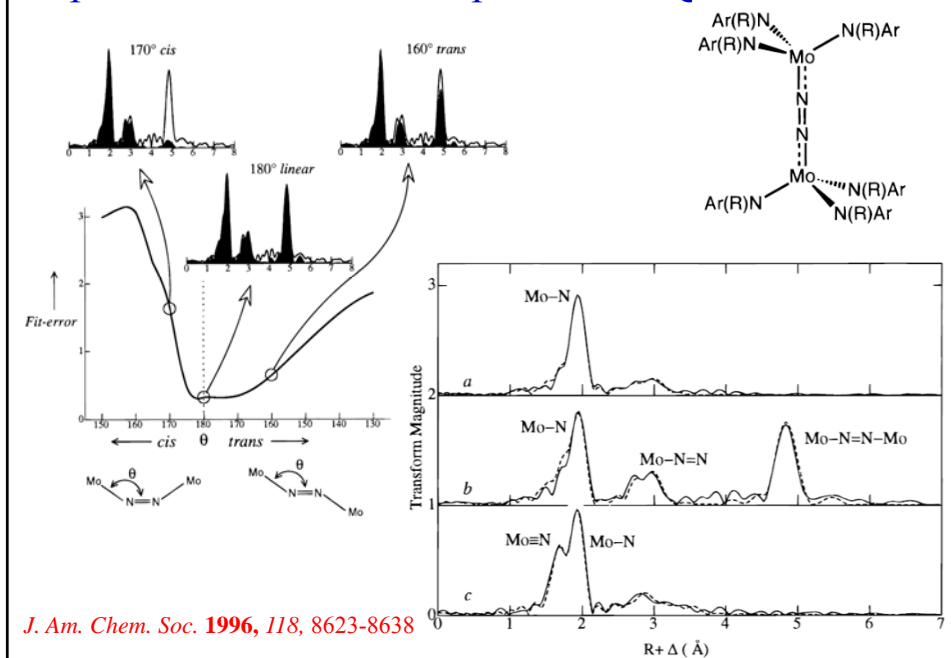


Scattering probability as a function of scattering angle

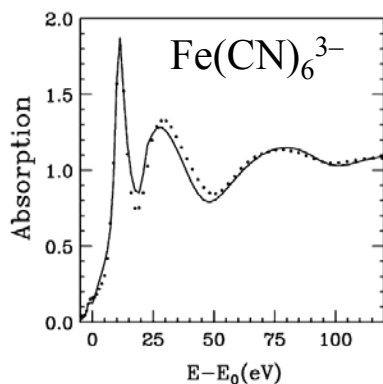


Barton and Shirley, *Phys. Rev. B* **1985**, 32, 1892

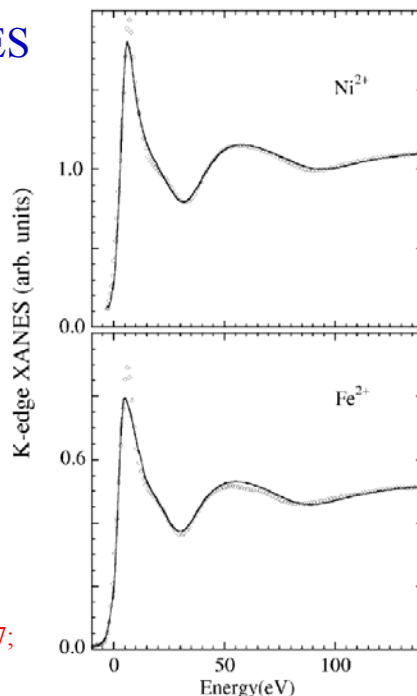
Importance of linear multiple scattering



MXAN can simulate XANES spectra (at least for some compounds under some conditions)

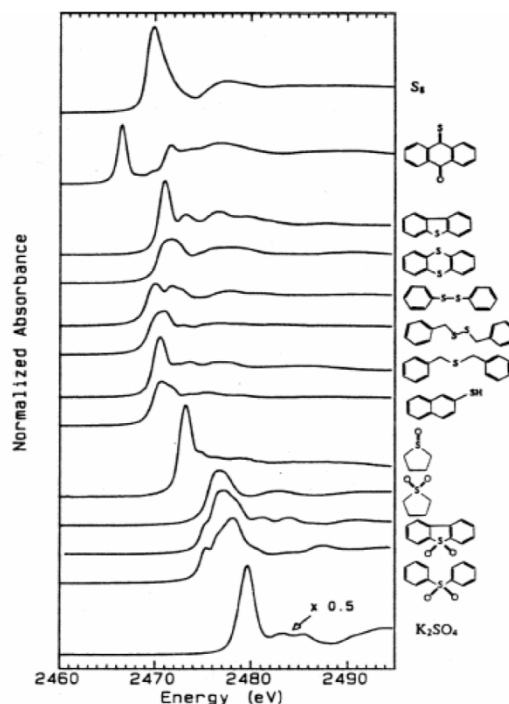


Benfatto et al, *J. Synchr.Rad.* **2003**, *10*, 51-57;
J. Am. Chem. Soc. **2004**, *126*, 15618-15623

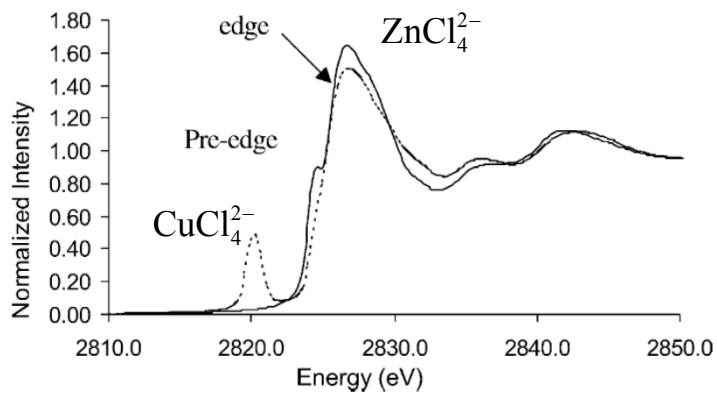


XANES studies
are not limited
to metals

George and Gorbaty, *J. Am. Chem. Soc.* **1979** *101*, 3182

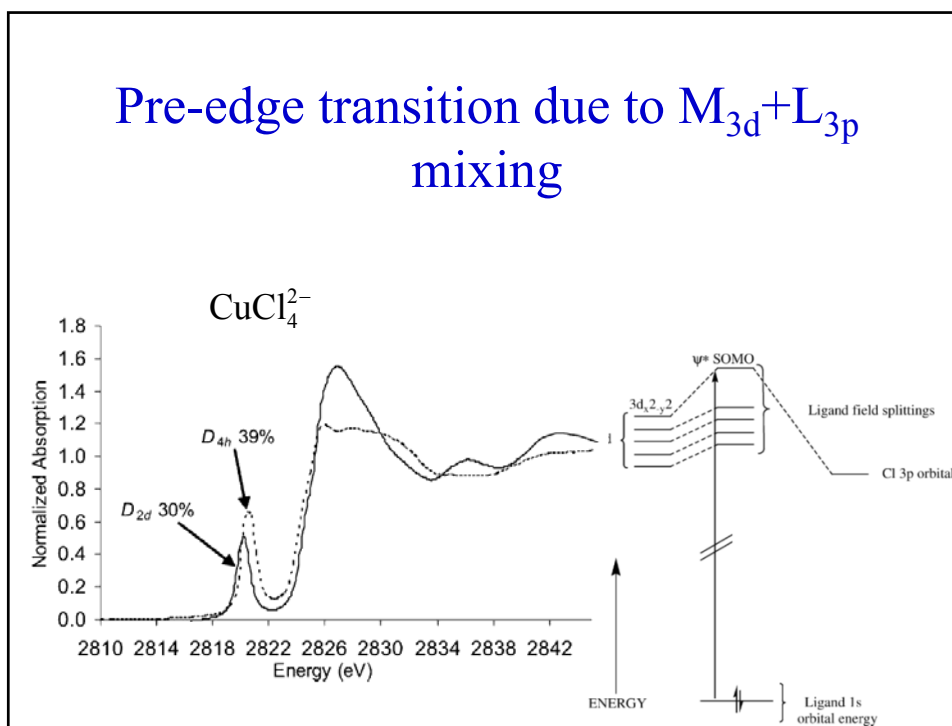


Ligand edges show pronounced
dependence on metal identity

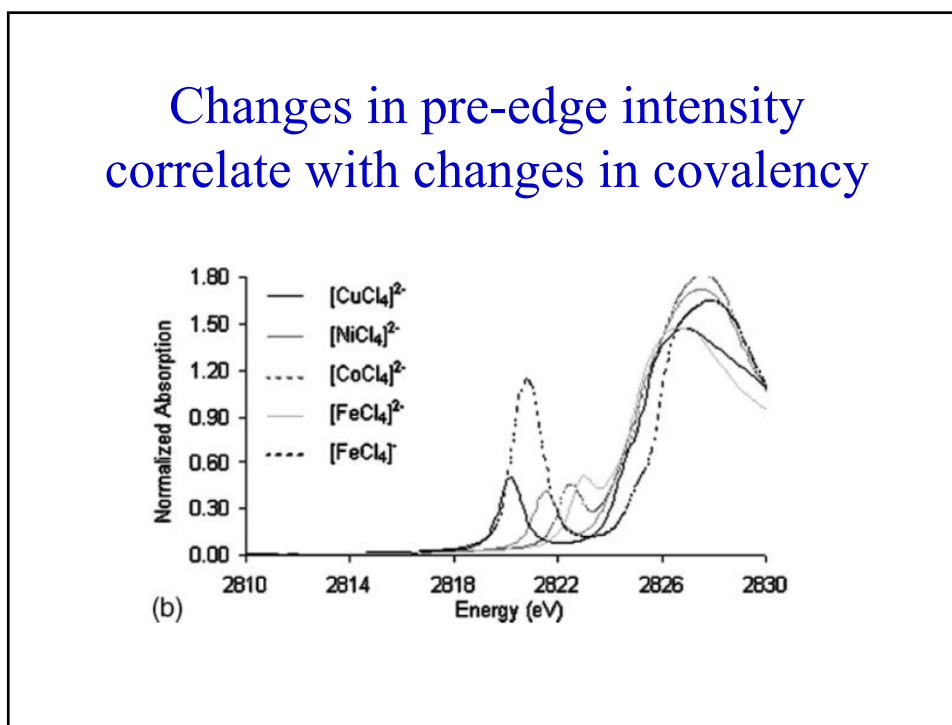


Hedman, et al., *J. Am. Chem. Soc.* **1990**, *112*, 1643

Pre-edge transition due to $M_{3d}+L_{3p}$ mixing

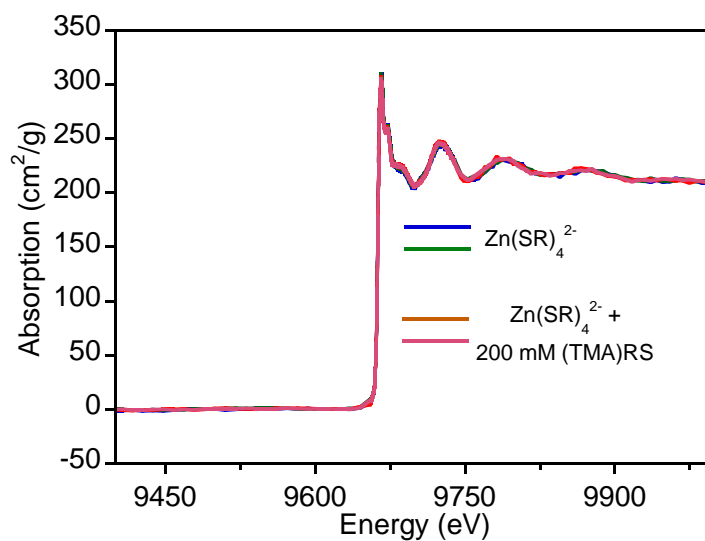


Changes in pre-edge intensity correlate with changes in covalency

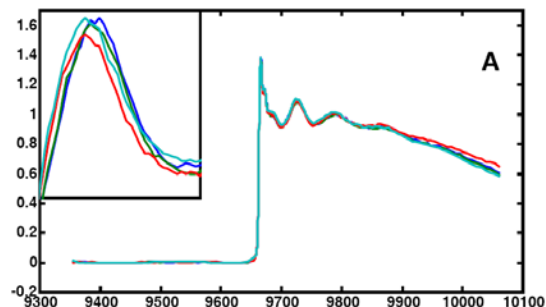


XANES (and potentially EXAFS) as a probe of solution structure

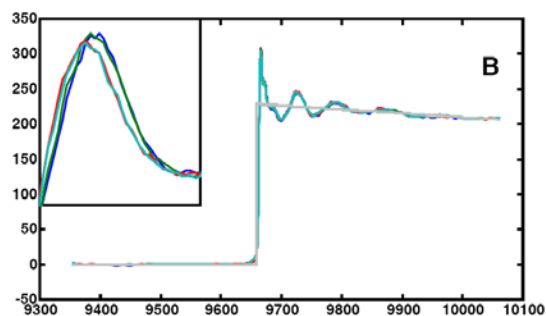
XANES spectra show only very small
changes with added thiolate



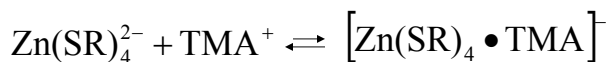
Conventional normalization misses changes in XANES



MBACK reveals subtle changes when thiolate is added



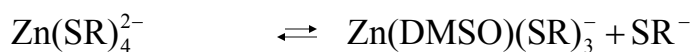
Equilibria for $\text{Zn}(\text{SPh})_4^{2-}$ in DMSO



$$K_{\text{IP}} = 13 \pm 4 \text{ M}^{-1}$$



$$K_{\text{D,IP}} = 0.01 \pm 0.009 \text{ M}^2$$

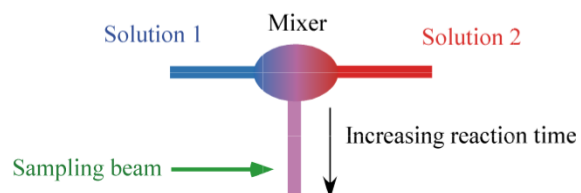


$$K_{\text{D}} = 0.13 \pm 0.12 \text{ M}$$

For 5 mM Zn, >75% dissociation

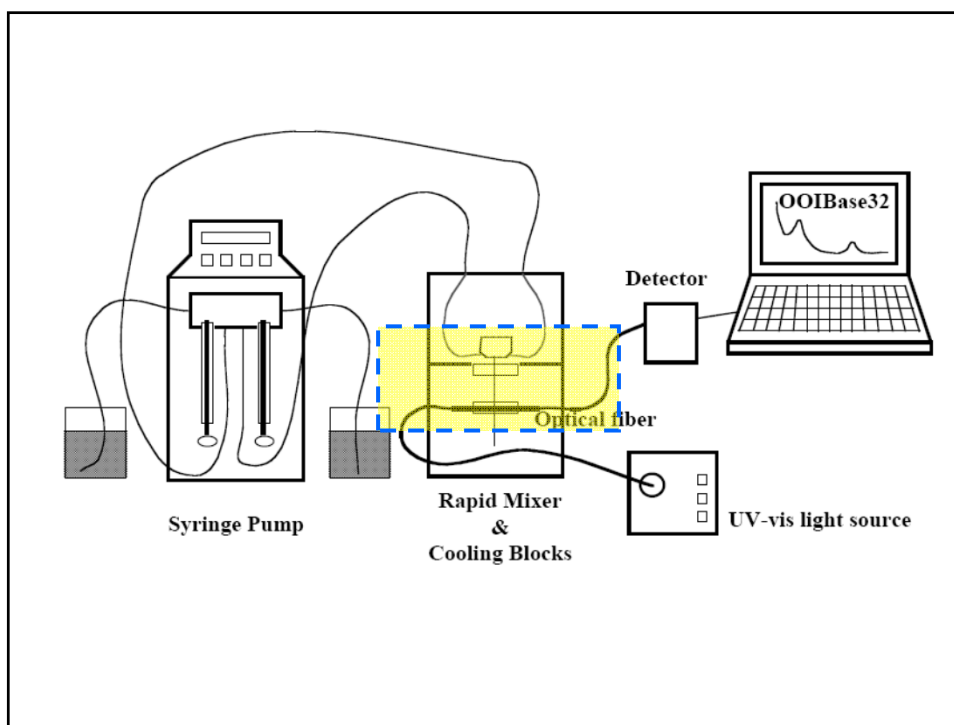
Wilker and Lippard, *Inorg. Chem.* (1997) **36**, 969.

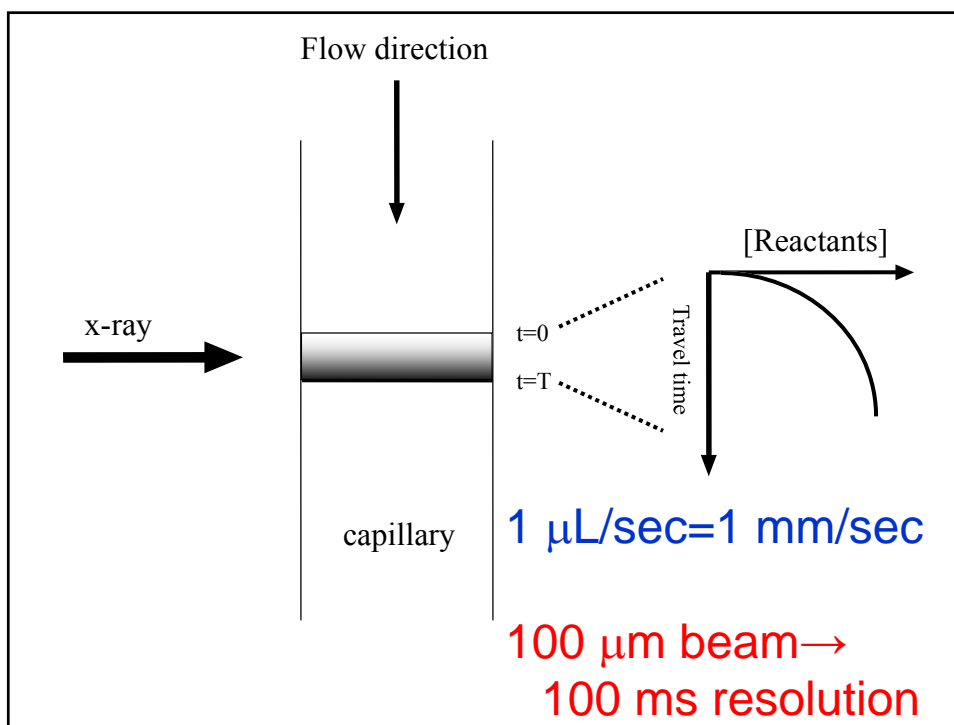
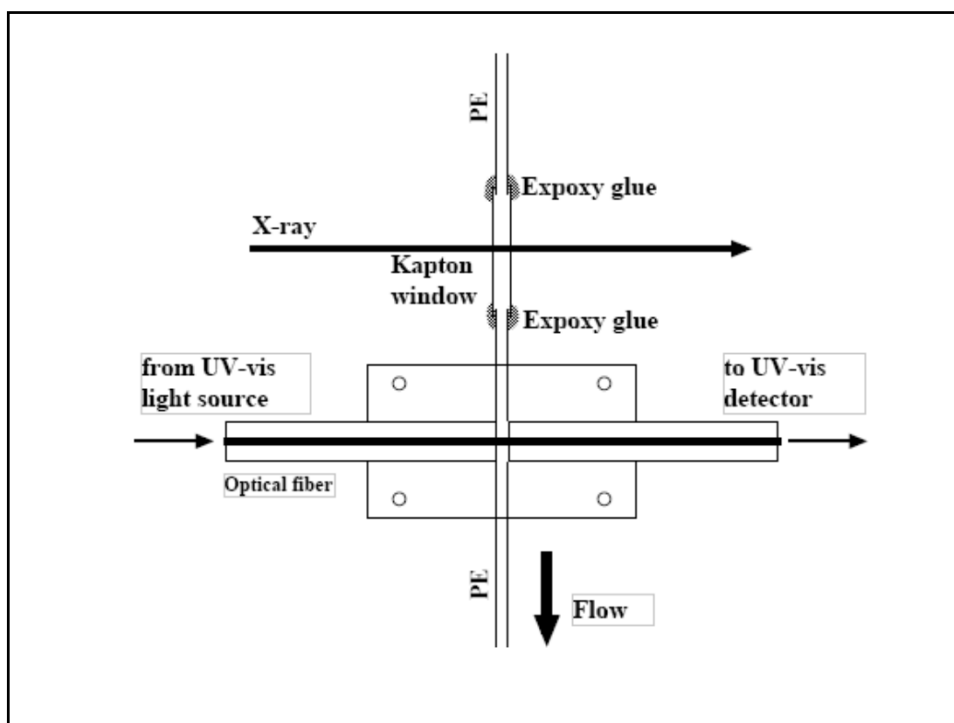
Flow system can be used for time resolved measurements

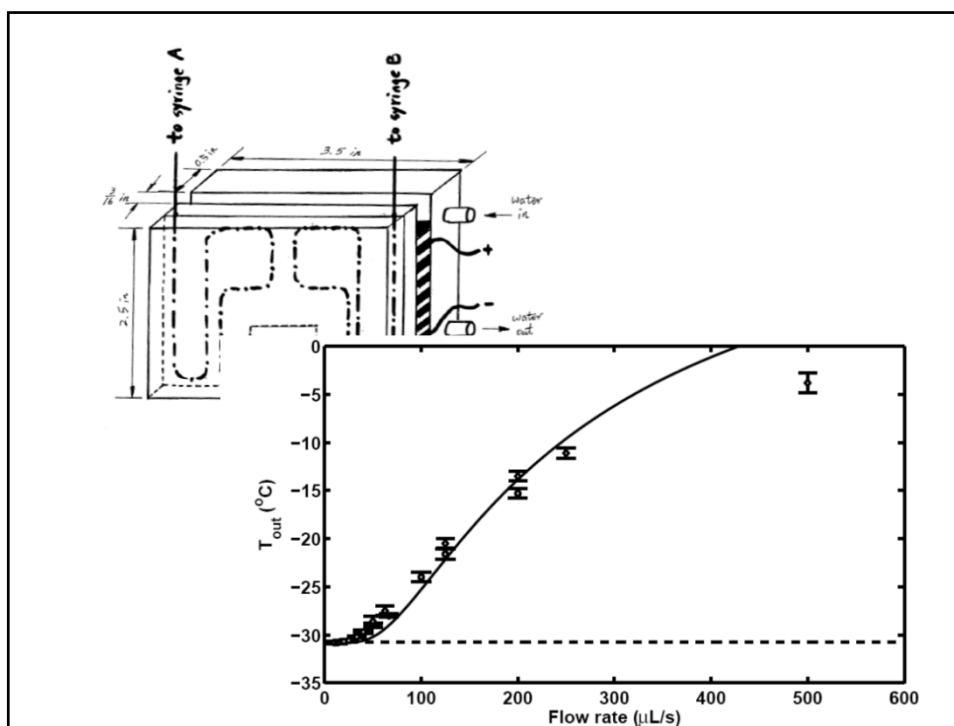


Requirements (for reasonable sample volumes):

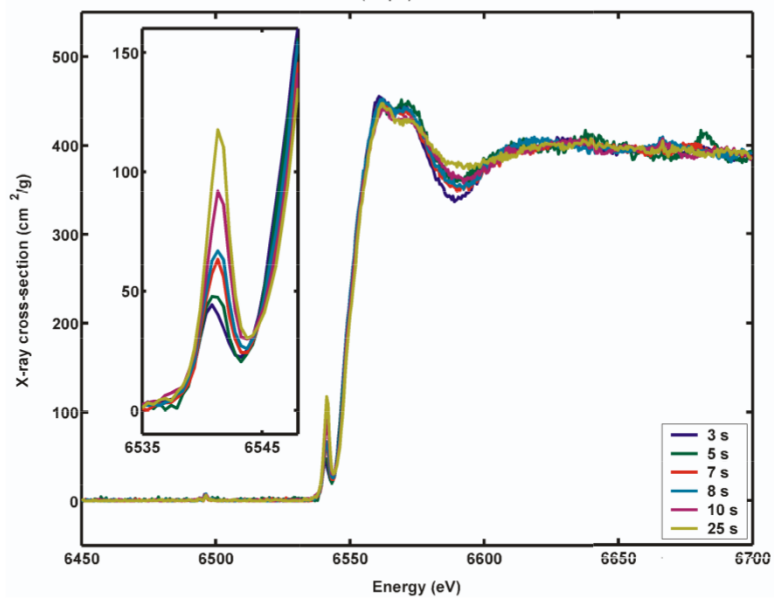
- Rapid scanning
- Small sample (i.e., small beam)



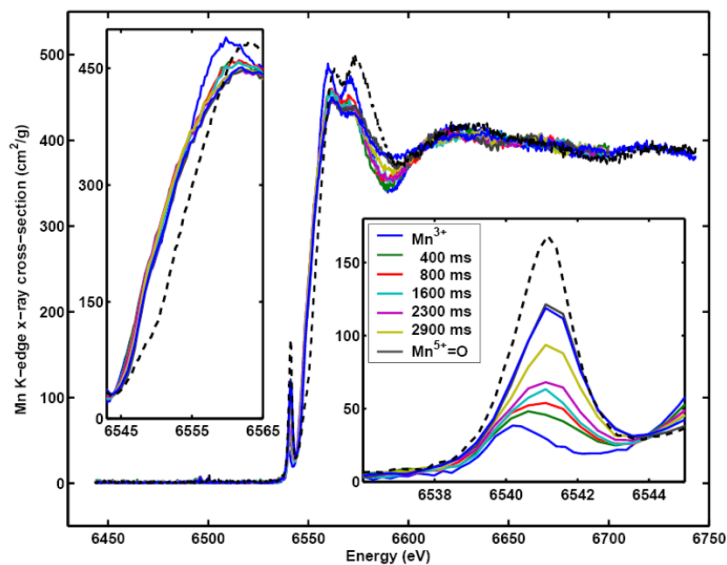




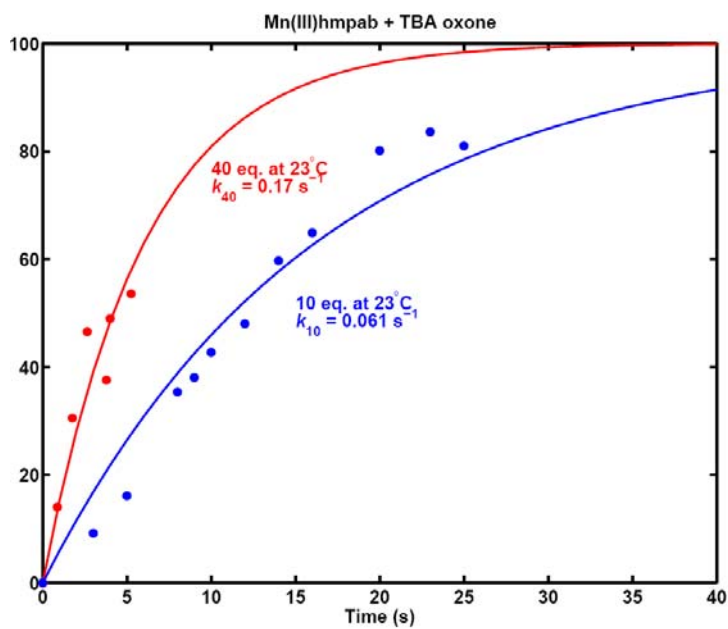
Oxidation of Mn(III)hmpab by oxone is slow at 0° C



Oxidation is significantly faster at room temperature

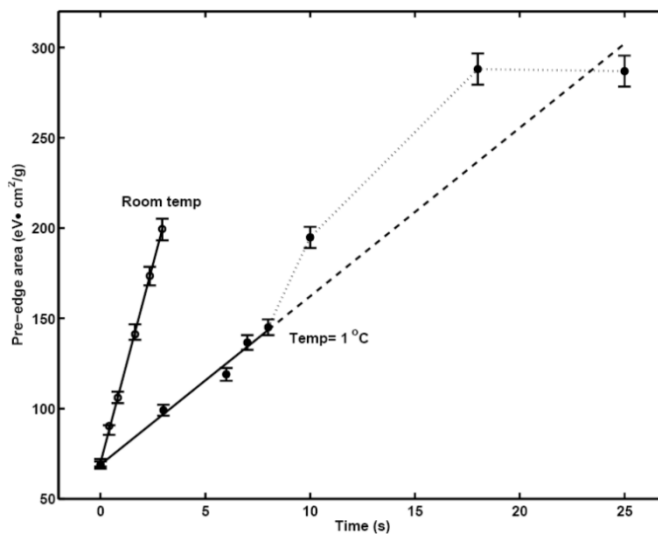


Reaction appears to be first order in Mn and oxone

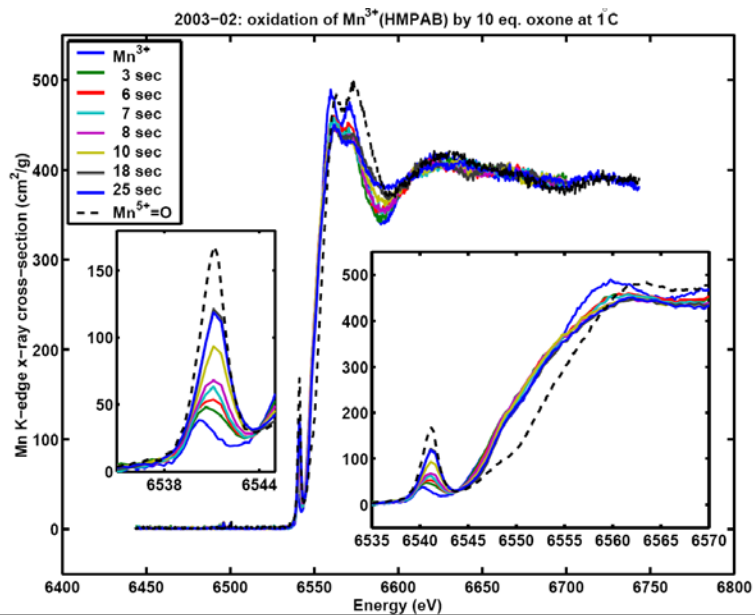


Initial rate is temperature dependent

$$\Delta G^\ddagger = 23 \text{ kJ/mol}$$

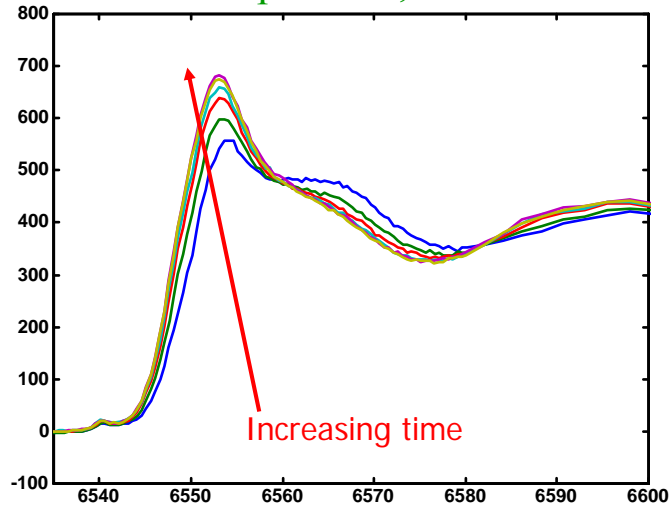


However, product that is formed is Mn(IV)=O not Mn(V)=O

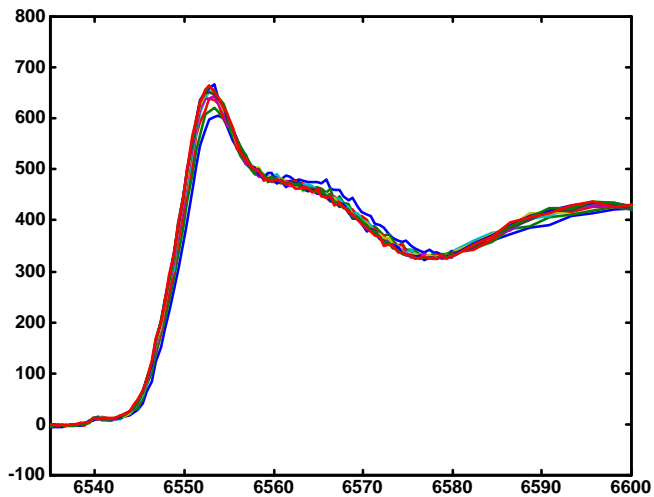


Mn(III) shows significant radiation damage

Room temperature, 30 minute scans



Low temperature (4K) reduces *but does not eliminate* radiation damage



Low temperature can't be used if thermochromic

Flowing fluid samples *can* prevent radiation damage

$\text{Mn}^{3+}(\text{salpn})(\text{acac})$ in Acetone + 15% H_2O

